Indian J. Phys. 47, 167-176, (1973)

Convective Couette-Poiseuille shear flow with massive blowing

B. C. CHANDRASEKHARA, S. B. LALSANGI*, N. RUDRAIAH

Department of Mathematics (Postgraduate Studies) Visvesvaraya College of Engineering, Bangalore University, Bangalore-1, India

(*Received* 9 *May* 1972)

This is a study of the effect of strong blowing on the free convective flow between a porous sliding cylinder and a porous stationary cylinder when the system is oriented at different angles to the horizontal. Closed form solutions are obtained in a unified form applicable to either two-dimensional or axisymmetric flow including heat transfer. A detailed examination of the solution in the massive blowing regime is also made and the analysis reveals that the solution possesses two layered structure and the shear layer blow off from the blown surface occurs at sufficiently large injection Reynolds number. Further it is found that for large values of Grashof number the pressure distribution exhibits a marked change.

1. INTRODUCTION

The massive blowing with thermal convection plays an important role in aerodynamics and in transpiration cooling. More specifically, the problem of strong blowing into aerodynamic body flow fields, where the injection rates are well above those permitted by the boundary layer assumptions, is currently under extensive study by many investigators (Inger 1969).

The problem of thermal convection across porous boundaries, maintained at different temperatures, consists of transport of heat by the interaction of moving and injected fluids in which the local variation of temperature, and hence the density, sets up the buoyancy force that itself modifies the flow pattern. Further when injected and moving fluids are of different densities, added to the local variation of temperature, we should take into account the buoyancy force due to the local variation of concentration. In the present paper, however, we assume that the densities of injected and moving fluids are the same and hence the effect of concentration is neglected. The combined effect of local variation of temperature and concentration will be presented elsewhere. In general, problems involving the interaction of velocity, density and other fields are mathematically complicated. Under such circumstances only special and simple categories of forced and natural convection have been studied theoretically in detail. For forced convection the velocity is usually large and the density of fluid is regarded

K. L. E.'s S. Nijalingappa College, Bangalore.

as totally unaffected by the transport of heat. Mathematically the problem reduces to finding the temperature distribution due to heated or cooled boundaries in a specified velocity field. For natural convection the motion of fluid is caused solely by buoyancy force, due to the action of some field of force on the unevenly heated fluid and the velocities established are usually small.

Recently Inger (1969) has examined the effect of strong blowing on the forced convective flow between a sliding porous cylinder and a porous stationary cylinder. He finds that shear layer blow off from the blown surface occurs for sufficiently strong blowing and the solution in the massive blowing regime consists oftwo layered structure. The aim of the present problem is to study the effect of strong blowing on the free convective flow between a porous sliding and a porous stationary cylinder oriented at different angles to the horizontal. The asymptotic nature of the solution when injection Reynolds number is very large is also discussed.

2. Formulation of the Problem

A uniform incompressible fluid of density ρ and viscosity μ flows through a channel formed by two infinitely long porous concentric cylinders of radii r_0 and r_i, oriented at an angle θ to the horizontal. The outer cylinder slides with an uniform axial velocity $u = U$ relative to the stationary inner cylinder and the cylinders are maintained at temperatures T_i and T_0 (figure 1) The fluid is injected radially with a variable velocity, $v = A/r$ through the inner cylinder, whereas the magnitude at the inner cylinder is v_w. Since the flow is axisymmetric and two dimensional in nature it follows that all the physical quantities in connection

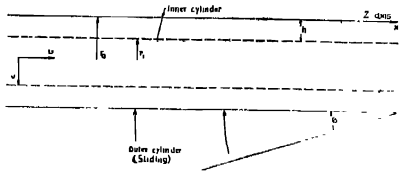

Figure 1. Physical model.

with the flow are functions of r only except for pressure which may have an arbitrary constant axial pressure gradient. The density is assumed to be of the form $\rho = \rho_0\{1-\alpha_1(T-T_0)\}$ where α_1 is the coefficient of thermal expansion of the fluid. The governing equations of motion and energy for the Boussinesq fluid, in terms of normalized distance $\eta = (r-r_i)/(r_0-r_i)$, velocity $\bar{u} = u/U$, $\bar{v} = v/v_w$, pressure $\bar{P} = p/\rho v_w^2$, temperature $\bar{T} = (T-T_0)/(T_i-T_0)$ and transverse curvature parameter $\lambda = h/r_i$, such that $r/r_i = (1+\lambda\eta)$, become

$$(1+\lambda\eta)\bar{v} = 1 \qquad \ldots (1)$$

$$\frac{d^2\bar{u}}{d\eta^2}(1+\lambda\eta)^2+(1+\lambda\eta)(\lambda-R_b)\frac{d\bar{u}}{d\eta}=(\Lambda-\epsilon\sin\theta)(1+\lambda\eta)^2+\frac{G\sin\theta}{R}\bar{T}(1+\lambda\eta)^2 \quad \ldots (2)$$

$$\bar{v}\frac{d\bar{v}}{d\eta}=-\frac{d\bar{P}}{d\eta}+\frac{\cos\theta}{F_t}-\frac{G\cos\theta}{R_b^2}\bar{T} \quad \ldots (3)$$

$$\frac{d^2\bar{T}}{d\eta^2}(1+\lambda\eta)+(\lambda-PR_b)\frac{d\bar{T}}{d\eta}=0 \quad \ldots (4)$$

The boundary conditions are

$$\left.\begin{aligned}&\bar{u}(0)=\bar{T}(1)=0\\&\bar{v}(1)=\bar{u}(1)=\bar{T}(0)=1\\&\bar{P}(1)=P_0/\rho v_w^2\end{aligned}\right\} \quad \ldots (5)$$

Where $R_b=\frac{v_w h}{\nu}$ is the injection Reynolds number

$R=\frac{Uh}{\nu}$ is the Reynolds number based on sliding velocity

$P=\frac{\nu}{K}$ is the Prandtl number

$G=\frac{gh^3\alpha_1(T_1-T_0)}{\nu^2}$ is the Grasshoff number

$F_t=\frac{v_w^2}{gh}$ is the Froude number based on injection velocity

P_0 is the atmospheric pressure

$\Lambda=\frac{h^2}{\rho_0 U\nu}\frac{dp}{dx}$ is the axial pressure gradient

$\epsilon=R/F_s$

$F_s=\frac{U^2}{gh}$ is the Froude number based on sliding velocity.

The momentum equation (3) has purely an inviscid character due to the nature of injection velocity $\bar{v}=1/(1+\lambda\eta)$. In the energy equation (4) the term due to viscous dissipation is not present, for we are dealing with free convection problems, where the velocities involved are small. It is of interest to note that in the present problem due to the nature of the injection velocity the energy

equation (4) is decoupled from the axial velocity and the solution for $\bar{T}$ can be obtained directly.

3. Temperature Distribution

Since the energy equation is not coupled with the velocity, the solution for $\bar{T}$ is obtained directly and the solution for $\bar{T}$ satisfying the boundary conditions (5) is

$$\bar{T} = 1 - \left\{ \frac{(1+\lambda\eta)^{P\alpha} - 1}{S_1} \right\} \tag{6}$$

where $$S_1 = (1+\lambda)^{P\alpha} - 1 \quad \text{and} \quad \alpha = R_b/\lambda$$

The temperature distribution is drawn in figures (2) and (3) for different values of P, R_b and λ. It is observed from figure (2) that for large values of R_b and small values of λ the profiles are pushed towards the moving boundary and this effect is more pronounced for $P = 1.5$ (figure 3). The heat transfer from the moving surface (*i.e.*, the Nusselt number N_0),

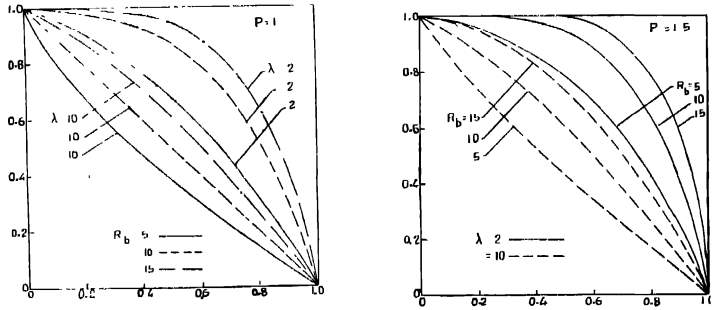

Figures 2, 3. Temperature profiles.

where $$N_0 = \frac{PR_b(1+\lambda\eta)^{P\alpha-1}}{S_1} \tag{7}$$

is evaluated numerically for different values of R_b and λ and is shown in figure 4. It is seen that for small values of λ(*e.g.* $\lambda = 2$), N_0 increases linearly with R_b whereas, for large values of λ, N_0 exhibits increasing tendency, but the magnitude of N_0 is small compared with the magnitude of N_0 when $\lambda = 2$. From this it is clear that increase in transverse curvature parameter decreases the heat transfer from the moving surface.

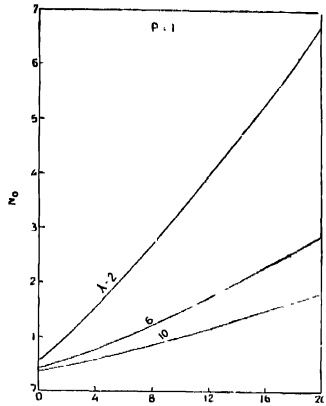

FIG 4

Figure 4 Variation of N_0 *vs* R_b.

4. Velocity Distribution

The expressions for axial velocity and axial shear stress at the inner cylinder obtained from equation (2) using (5) and (6) are

$$\bar{u} = C\{(1+\lambda\eta)^{\alpha}-1\}+X\{(1+\lambda\eta)^{2}-1\}-Y\{(1+\lambda\eta)^{P\alpha+2}-1\} \quad \ldots \quad (8)$$

$$\left(\frac{d\bar{u}}{d\eta}\right)_{\eta=0} = 2(X-Y)\lambda+\alpha(C-PY)\lambda \quad \ldots \quad (9)$$

$$C = \frac{1}{S_2}\,[1-X\{(1+\lambda)^{2}-1\}+Y\{(1+\lambda)^{P\alpha+2}-1\}]$$

$$X = \frac{1}{RSS_1}\,[(\Lambda-c\sin\theta)RS_1+GSS_1\sin\theta+G\sin\theta]$$

$$Y = \frac{G\sin\theta}{RS_1\{(P\alpha+2)^{2}\lambda^{2}-\alpha\lambda^{2}(P\alpha+2)\}}$$

$$S = 4\lambda^{2}-2R_b\lambda$$

$$S_2 = (1+\lambda)^{\alpha}-1$$

Equation (8) in the limit $\lambda \to 0$ reduces to the two-dimensional flow result and is given by

$$\bar{u} = A(\exp R_b\eta - 1) - \frac{X_1\eta}{R_b} - Y_1(\exp PR_b\eta - 1) \qquad \ldots \quad (10)$$

where $$A = \frac{1}{\exp R_b - 1}\left[1 + \frac{X_1}{R_b}\, Y_1(\exp PR_b - 1)\right],$$

$$X_1 = \Lambda - c\sin\theta + \frac{G\sin\theta}{R} + \frac{G\sin\theta}{RS_1}, \quad Y_1 = \frac{G\sin\theta}{PR\bar{R}_b^2(P-1)(\exp P\bar{R}_b - 1)}$$

Some typical velocity profiles are illustrated in figures (5), (6) and (7). Figure (5) illustrates the effect of increase in injection Reynolds number R_b in the absence

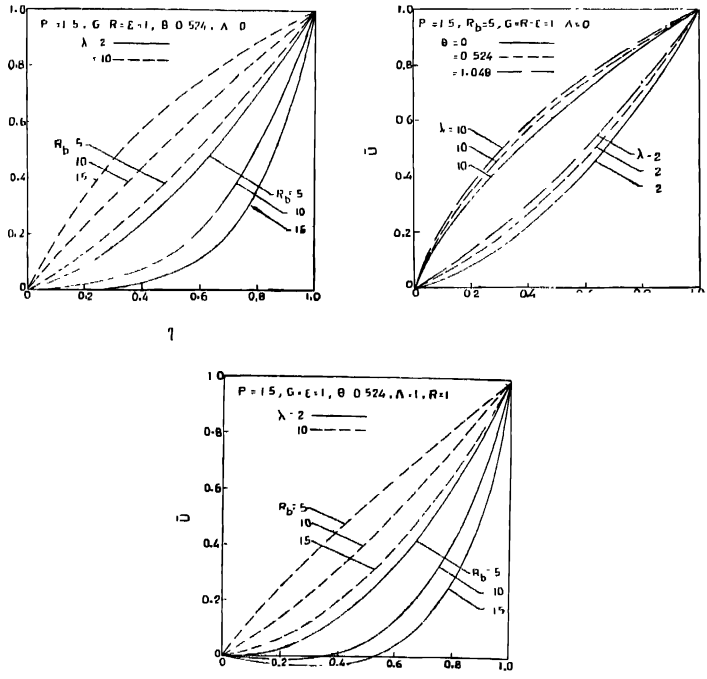

Figures 5, 6, 7. Typical axial velocity profiles.

of axial pressure gradient, for known values of other parameters It is observed that for small values of λ, increase in R_b pushes the boundary layer towards the sliding cylinder, whereas, for large values of λ the opposite behaviour is observed. Figure 6 illustrates the effect of increase in the angle of orientation on the axial velocity. In the case of adverse pressure gradient (*i.e.* $\Lambda > 0$, figure 7) the axial velocity exhibits flow reversal for small values of λ as R_b is increased The physical reason for this is that the dragging action of the faster layers exerted on fluid particles in the neighbourhood of the stationary wall will be reduced due to the adverse pressure gradient and this dragging action is insufficient to overcome the influence of strong adverse pressure gradient The critical value of Λ for separation, *i e* $(\mathrm{d}\bar{u}/\mathrm{d}\eta)_{\eta=0}$, is obtained from equation (8) and is given by

$$Y\{\lambda(P\alpha-2)\}+(X_1)(2\lambda)-\frac{R_b}{2S_2}\,[1+(X_1)\{(1+\lambda)^2-1\}+Y\{(1+\lambda)^{P\alpha+2}-1\}]$$
$$\frac{R_b}{2S}\left[\frac{4\lambda}{R_b}-\frac{1}{S_2}\{(1+\lambda)^2-1\}\right] \tag{11}$$

Λ_{Sep} is drawn in figure 8 It is seen that blowing decreases Λ_{Sep} such that under strong blowing conditions flow reversal is caused by small adverse pressure gradients for small values of λ. However, increase in λ delays flow reversal.

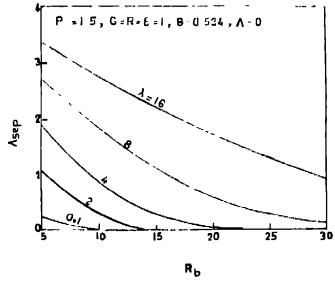

Figure 8. Axial pressure gradient variation for different values of λ.

5. Behaviour of the Solution in the Massive Blowing Limit

We shall now examine the structure of the solution in the massive blowing limit $R_b \gg 1$ and $P = 1$ for fixed λ. Barring the possibility $\lambda \lesssim 0(R_b)$ equa-

tions (8) and (9) can be written in the following forms appropriate to the limit

$$\bar{u} = [1-X'(2+\lambda)]\left[\exp\left\{-\alpha \ln\left(\frac{1+\lambda}{1+\lambda\eta}\right)\right\} - \exp\{-\alpha \ln(1+\lambda)\}\right] + X'\eta(2+\lambda\eta) \tag{12}$$

where

$$X' = \frac{1}{2R_b\bar{R}S_1}[R(\epsilon \sin\theta - \Lambda)S_1 + G \sin\theta + GSS_1 \sin\theta]$$

and

$$\left(\frac{d\bar{u}}{d\eta}\right)_{\eta=0} = R_b[1-X'(2+\lambda)] \exp\{-\alpha \ln(1+\lambda)\} + 2X' \tag{13}$$

These relations reveal that the wall shear and the axial velocity over some distance from the lower wall tend to vanish for sufficiently large values of R_b, suggesting that the shear layer becomes effectively blown off the surface. Further examination of these solutions reveal that the solution for axial velocity possesses two-layered structure whose nature depends on the axial pressure gradient Λ, θ and G. We can identify an outer solution in each of equations (12) and (13) which is valid in the entire flow region except for a small thin region near the moving surface, since the first term on the right side of each equation (12) and (13) is exponentially small for $R_b \gg 1$. This outer solution becomes a constant shear motion irrespective of Λ is present or not and depends algebraically on R_b^{-1}. This type of motion is qualitatively similar to flows studied by Yaun (1956), Terrill (1965), Shresta (1967) and Rudraiah & Chandrasekhara (1969). The inner solution which is valid in the region near the moving surface is obtained by introducing an inner variable $z = \alpha \ln((1+\lambda)/(1+\lambda\eta))$ into equation (12) and it takes the form

$$\bar{u} = e^{-z} - X'(2+\lambda)(e^{-z}-1) + 0(R_b^{-2}) + \ldots \tag{14}$$

where

$$z(\eta = 1) = 0, \quad z(\eta = 0) \to \infty$$

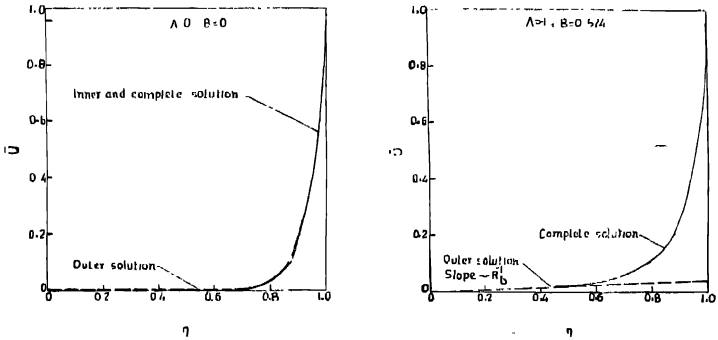

Figures a), 9(b). Schematic of asymptotic massive blowing solution.

This inner solution is independent of Λ and other parameters in leading asymptotic expansion. To the order of approximation involved this inner solution is the complete solution throughout the channel when Λ, θ and G are zero, since the leading term satisfies both boundary conditions $\bar{u}(z=0)=1$ and $\bar{u}(z=\infty)=0$. When $\Lambda \leqslant 0$ the full solution is obtained by matching the outer and inner solutions, which is qualitatively illustrated in figure 9.

6. Pressure Distribution

Solving equation (3) we obtain the expression for $\bar{P}_0-\bar{P}$ in the form

$$\bar{P}_0-\bar{P} = \frac{1}{2}\left\{\frac{1}{(1+\lambda\eta)^2}-\frac{1}{(1+\lambda)^2}\right\}+\frac{\cos\theta}{F_t}(1-\eta)-\frac{G\cos\theta}{R_b{}^2}(1-\eta)$$

$$-\frac{G\cos\theta}{R_b{}^2 S_1}(1-\eta)+\frac{G\cos\theta}{R_b{}^2 S_1\lambda(P\alpha+1)}\{(1+\lambda)^{P\alpha+1}-(1+\lambda\eta)^{P\alpha+1}\} \quad \ldots (15)$$

Expression (15) has been evaluated numerically for different values of R_b, θ and G and is represented in figures 10, 11 and 12. From figure 10 we find that increase in R_b increases the pressure slightly for known values of other parameters. It is seen that increase in the angle of orientation (figure 11) decreases the pressure for given values of other parameters. We note that even though the Grashof number has no significant effect on the velocity profiles, it has a marked effect on the pressure distribution. This is evident from figure 12 where for $G=100$, $\bar{P}_0 > \bar{P}$, whereas, for $G=1000$, $\bar{P} > \bar{P}_0$

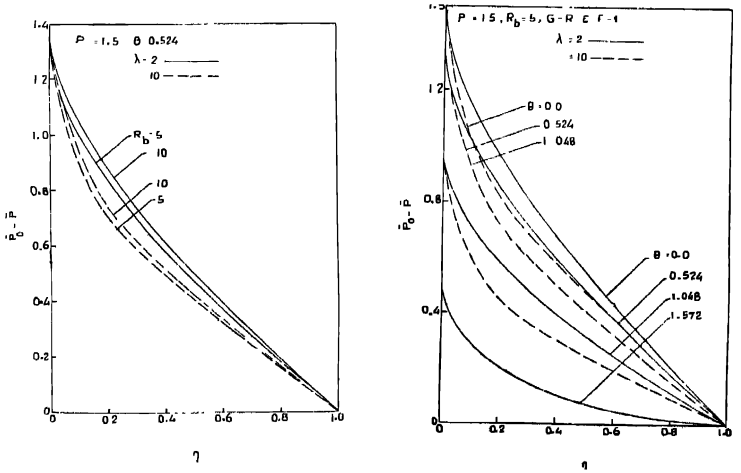

Figures 10, 11, Pressure variation across the channel.

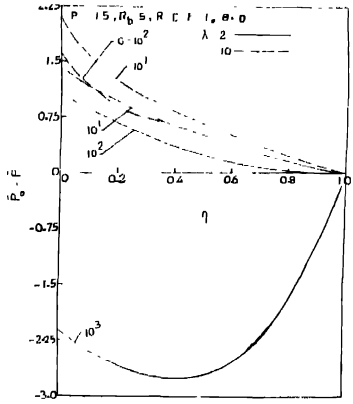

Figure 12 Pressure variation across the channel.

7. Conclusions

The present investigation is devoted to the study of the effect of strong blowing into a viscous Boussinesq fluid, considering an idealized Couette-Poiseuille shear flow. This simple model exhibits all the basic physical trends that are associated with injection into boundary layers. Further, the following interesting features are observed.

1) The existence of a two layered structure of the solution in the massive blowing limit whose nature depends on G and θ

2) Change in pressure distribution for large values of Grasshoff number, G. These results have significant implications involving analysis of massive blowing in more realistic flow configurations.

References

Inger G. R 1969 *Phys Fluids* **12**, 1741.
Rudraiah N. & Chandrasekhara B. C 1969 *Bull. Aca. Sci. Georgian* SSR **53**, 285.
Shrestha G. M. 1967 *QJMAM* **20**, 233.
Terrill R M. 1965 *Aeronaut. Quart.* **16**, 323
Yaun S. W. 1956 *J. Appl. Phy.* **27**, 267.